AGU ADVANCING EARTH AND SPACE SCIENCE

Geophysical Research Letters®

RESEARCH LETTER
10.1029/2021GL093415

Key Points:

- Mechanistic bedrock erosion laws can be upscaled from point to patch and minute to year
- Discharge-based erosion models are only reliable in their calibration range
- Exceptional events dominate long-term bedrock erosion

Supporting Information:

Supporting Information may be found in the online version of this article.

Correspondence to:

A. R. Beer,
alexander.beer@uni-tuebingen.de

Citation:

Beer, A. R., & Turowski, J. M. (2021). From process to centuries: Upscaling field-calibrated models of fluvial bedrock erosion. *Geophysical Research Letters*, *48*, e2021GL093415. https://doi.org/10.1029/2021GL093415

Received 24 MAR 2021
Accepted 22 AUG 2021

From Process to Centuries: Upscaling Field-Calibrated Models of Fluvial Bedrock Erosion

Alexander R. Beer[1,2,3] and Jens M. Turowski[4]

[1]Swiss Federal Institute for Forest, Snow and Landscape Research WSL, Birmensdorf, Switzerland, [2]Department of Environmental System Science, ETH Zurich, Zurich, Switzerland, [3]Department of Geosciences, University of Tuebingen, Tuebingen, Germany, [4]Helmholtzzentrum Potsdam, German Research Centre for Geosciences GFZ, Potsdam, Germany

Abstract Fluvial bedrock erosion formulas lack validation over space and time. We explore the performance of field-calibrated models at the patch-scale ($<1m^2$) and from minutes to centuries. At the hour to annual scales (in 1-min resolution), we verify predictions using linked discharge, bedload transport and at-a-point erosion, together with spatial erosion from a mountain streambed. Local and spatial erosion linearly scale with bedload mass. The unit stream power model (*USP*) fails to describe erosion dynamics without a threshold for its onset. Extrapolating over the decadal scale (14 years of discharge and bedload data), scaled models predict up to 12% of erosion for two exceptional floods. Erosion predictions for a bi-centennial discharge varied over four orders of magnitude (extrapolated from 32.5 years discharge and 16 years bedload data at 10-min resolution). Bi-centennial erosion predictions summing up to 1 m for bedload models versus 0.1 m for *USP* highlight the likely dominance of large events in setting long-term erosion under sediment-starved conditions.

Plain Language Summary Bedrock channel erosion drives whole mountain landscape generation, since bedrock beds are the baseline of hillslopes, and their alteration affects catchment sizes and particular and dissolved matter routing. For channel erosion simulations, commonly, water discharge-based models are used, despite that sediment impacts seem to be the actual erosion agents. Though, all these models are generally calibrated to specific data in time and space and it is unknown in how far they are feasible to predict channel evolution under diverse other spatio-temporal scales. We assess model scalability from minute to century timescales, using unique, combined field data of discharge, bedload, and (partly) bedrock erosion in 1–10-min resolution. Erosion linearly scales with impacting bedload mass over time and (local) space-discharge is not a good predictor for it. For our steep pre-Alpine creek, two large events in 14 years would have accounted for 12% of the total erosion, highlighting the role of extreme bedload events for channel shaping. For centennial floods, bedload-dependent models predict four orders of magnitude higher erosion than solely discharge-dependent models. For a ~200-year period, accounting for bedload would result in 1-m bedrock erosion versus 0.1 m when only accounting for discharge. Predictability of discharge-driven models thus strongly depends on their calibration period.

1. Introduction

Stream channels represent a crucial actor in mountain regions, routing bio-physico-chemical fluxes from their watersheds. In actively eroding areas, these channels are typically constricted by bedrock boundaries, which adjust their geometry in an interplay of tectonics and climate (Egholm et al., 2013; Whipple et al., 2013). A range of models are available to predict fluvial bedrock erosion rates, from the empirical shear stress and stream power models (Howard & Kerby, 1983; Seidl & Dietrich, 1992) to mechanistic process models describing bedrock abrasion by particle impacts (Auel et al., 2017; Lamb et al., 2008; Sklar & Dietrich, 2004) or by fluvial plucking (Chatanantavet & Parker, 2009; Hancock et al., 1998). While process research shows that bedrock erosion is driven by the impacting sediment (Beer et al., 2017; Cook et al., 2013; Inoue et al., 2014; Jacobs & Hagmann, 2015; Mueller-Hagmann et al., 2020), large-scale modeling of channel morphodynamics and landscape evolution commonly apply stream-power-based erosion formulas, which depend on discharge instead of sediment transport (Barnhart et al., 2020).

Due to the lack of data, model-parameters in such simulations generally are calibrated to specific spatial and temporal scales, based on arithmetic means of forcing variables or based on values exceeding likely dominant thresholds (e.g., discharge or excess discharge; Sklar & Dietrich, 2006; Tomkin et al., 2003; van der Beek & Bishop, 2003). They may also be based on some fundamental values like effective discharge (i.e., the discharge most effective in the long-term transport of sediment; Wolman & Miller, 1960). These models are then applied on other temporal and spatial scales. However, given that fluvial sediment transport and bedrock erosion are non-linear threshold processes, and that extreme and exceptional events may dominate long-term river incision behavior, calibration using arithmetic means cannot be expected to be representative for periods other than the ones used for calibration (e.g., Deal et al., 2017; Kirchner et al., 2001; Lague, 2010; Lague et al., 2003). Hence, it is currently unknown to what extent locally calibrated bedrock erosion models can be applied to diverse temporal and spatial scales (Lague, 2010; Whipple & Tucker, 1999). This implies that many equations and parameters, for example, used in landscape evolution models, carry an unknown uncertainty that may be substantial (Turowski, 2012).

To address this uncertainty and to make informed choices of model selection, calibration procedures, and parameter values, spatio-temporally high-resolution and linked field data are needed, including observation periods of different length and spanning a range of possible forcing parameter values. Here, we study validity, robustness, and behavior of the bedrock erosion model upscaling using a unique, spatio-temporally high-resolved field data set. Our aims are to (a) assess whether and how well event and point-calibrated process laws can successfully predict fluvial bedrock erosion rates over time scales of hours and years (validation), and (b) assess the implications of calibrated erosion model predictions over decades to centuries for the case of sediment-starved channel bed conditions (extrapolation).

2. Materials and Methods

2.1. Data Sets and Erosion Models

We used linked data of water discharge, bedload transport, and fluvial bedrock erosion from the Erlenbach sediment transport field observatory (Figure S1; Beer et al., 2015; Rickenmann et al., 2012). At the Erlenbach, a small and steep creek located in the Swiss Pre-Alps, discharge and bedload transport have been measured at 1-min resolution and with high accuracy since 2003, and are available at 10-min resolution since 1986. At-a-point erosion rates of smooth in-stream rock slabs equipped with erosion sensors have been recorded between 2011 and 2014. From October 2011 to June 2013 the surface of a concrete slab (tensile strength of 3.37 MPa) was also spatially surveyed six times at millimeter-resolution and submillimeter accuracy and precision (Text S1). These surveys confine five temporal data intervals (I–V) differing in length, cumulative discharge, total bedload transport, and spatial bedrock surface change (Table S1). For each individual data interval, we calculated "mean spatial slab-surface erosion values" *MSE* based on vertical changes of all surveyed slab points (Text S1). Additional 10 combined data intervals from joining adjacent intervals served to extend the time scale of the individual intervals and to check for linearity, though they do not add new data (Table S2).

Using the measured erosion-forcing parameters water discharge and bedload transport rate, we applied five different erosion models from the literature (Table 1; Beer & Turowski, 2015) to recalculate the observed *MSE*: (a) the unit stream power model *USP* (Howard, 1994) as the most popular erosion model; (b) an excess *USP* model version (*EUSP*, Sklar & Dietrich, 2006) with a threshold discharge for the onset of bedload motion; (c) the tools-only model (*TO*) (Beer & Turowski, 2015), in which the erosion rate is a power function of the bedload transport rate; (d) the saltation abrasion model without its suspension term (*SAws*) (Sklar & Dietrich, 2006), a fully mechanistic model including both sediment tools and cover effects; and (e) the revised saltation abrasion model *RSA* (Auel et al., 2017), a version of *SAws* without the onset of bedload motion, calibrated on up-to-date experimental data. Because no suspended load measurements are available for the Erlenbach, where bedload can be considered dominant (Rickenmann et al., 2012), we did not apply the total load model of Lamb et al. (2008). Mean model efficiency factors (k-factors) were calibrated by equating the predicted erosion to the measured *MSE* over the combined data interval span (interval II–V, neglecting interval I due to reasons explained below). These k-factors comprise aspects of both the streamflow's erosivity (its ability to erode) and the bedrock's erodibility (its susceptibility to be eroded; Sunamura, 2018) for the conditions of the Erlenbach measurements. For the planar concrete slab surface considered here, abrasion

Table 1
Applied Bedrock Erosion Models With Their Erosion Efficiency Factors k, Scaled to the Combined Data Interval II–V

Erosion model	Original reference	Common formula	Model scaling k-factor[a]	
Unit stream power (*USP*)	Howard (1994)	$E \sim \omega^{0.5}$	k_{USP}: 3.2×10^{-11}	(m min$^{0.5}$/kg$^{0.5}$)
Excess unit stream power (*EUSP*)	Sklar and Dietrich (2004)	$E \sim \omega_{ex}^{0.5}$	k_{EUSP}: 9.1×10^{-10}	(m min$^{0.5}$/kg$^{0.5}$)
Tools only (*TO*)	Beer and Turowski (2015)	$E \sim q_s^{1.0}$	k_{TO}: 1.8×10^{-9}	(m^2/kg)
Saltation abrasion without suspension (*SAws*)	Sklar and Dietrich (2006)	$E \sim ts_{ex}^{-0.5}\, C^{1.0}\, q_s^{1.0}$	k_{USP}: 2.6×10^{-9}	(m^2/kg)
Revised saltation abrasion (*RSA*)	Auel et al. (2017)	$E \sim C^{1.0}\, q_s^{1.0}$	k_{RSA}: 1.9×10^{-9}	(m^2/kg)

Note. E = erosion rate (m/min); $\omega = \rho_w g Q_w S/W$ = unit stream power (W/m^2), with water density ρ_w (kg/m^3), gravitational acceleration g (m/s^2), water discharge Q_w (m^3/s), channel bed slope S (−), and channel width W (m), ω_{ex} = excess unit stream power (W/m^3); q_s = bedload transport per unit channel width (kg/[m min]); $ts_{ex} = \tau^*/\tau^*_c - 1$ = excess transport stage (−), with $\tau^* = \rho_w HS/(\rho_s - \rho_w)D$ = nondimensional bed shear stress (−), water depth H (m), sediment density ρ_w (kg/m^3), and grainsixe D (m); $C = (1 - q_{s/s,c})$ = sediment cover factor (−), with $_{s,c}$ = bedload transport capacity per unit chanel width (kg/[m min]).
[a]Mean over combined data interval II–V.

has been determined as the dominant erosion process (Beer et al., 2015). Hence, the subsequent erosion scaling and predictions are restricted to this process and to the slab's position in the fixed, stable, and slightly over-steepened chute channel (Figure S1; Beer & Turowski, 2015).

2.2. Multi-Scale Model Performance Assessment

The Erlenbach data span four distinct temporal scales. Typical flood events have a duration of a few hours and we refer to these short, intra-event periods as the hour scale. For a 20*month* period (month to annual scale) detailed discharge, bedload transport, and at-a-point erosion data at 1*minute* resolution are available. During this period seven bedload transport events occurred that caused slab erosion, as indicated by three erosion sensors (*e*1–*e*3, Table S1; Beer & Turowski, 2015). These events allowed us to study transient model performance (cf. Gasparini et al., 2007), and to assess abrasion model plausibility over months to years using the linked measurements during the individual data intervals (Figure S2). Mean slab erosion rates *MSE* were contrasted with potential erosion driving parameters calculated for each data interval: (a) cumulative time, (b) cumulative discharge, (c) cumulative discharge exceeding a threshold for bedload transport (which we term "exceeding discharge"), (d) cumulative bedload time, and (e) cumulative bedload transport mass. Further, a distribution of 10 k-factors was calculated for each erosion model by scaling its predictions to each of the 10 individual data and combined data intervals (considering intervals II–V, only; Table S2). Each scaled model was then applied to predict erosion rates for the remaining data intervals it was not scaled to. This procedure yielded 90 predictions per model to assess general scaling robustness based on the deviations between predicted and measured slab erosion.

For the decadal time scales, which are largely lacking bedrock erosion measurements, we refer to 14 years of continuous discharge and bedload transport data at 1-min resolution (2003–2016, including the month to annual scale data from above) to assess potential slab erosion. This data set contains more than 7.3 million time stamps and includes two exceptional floods that occurred at the Erlenbach in the last 40 years (Turowski et al., 2013). We calculated potential slab erosion rates over this time, using the model calibrations from the month to annual scale and neglecting likely changes in the concrete slab morphology and their effects on erosion rates. We then compared how cumulative erosion predictions varied over orders of magnitude of observed discharges. On the centennial time scale, we used the longest observational data sets at the Erlenbach (discharge over 32.5 years and bedload transport over 16 years, available at 10-min resolution) to predict potential instantaneous erosion rates on the concrete slab. Here, we assume a fixed bed geometry for the measurement site's chute channel, which is designed for discharges exceeding 20 m^3. We fitted a gamma function to the magnitude-frequency distribution of discharge measurements over 32.5 years, and for the related bedload transport rates we constructed a rating curve based on 16 years of measurements (Text S3). Assuming that these relationships are representative for the long-term behavior of the Erlenbach, we extrapolated erosion predictions to assess model performance over discharge return times exceeding the observed time scales.

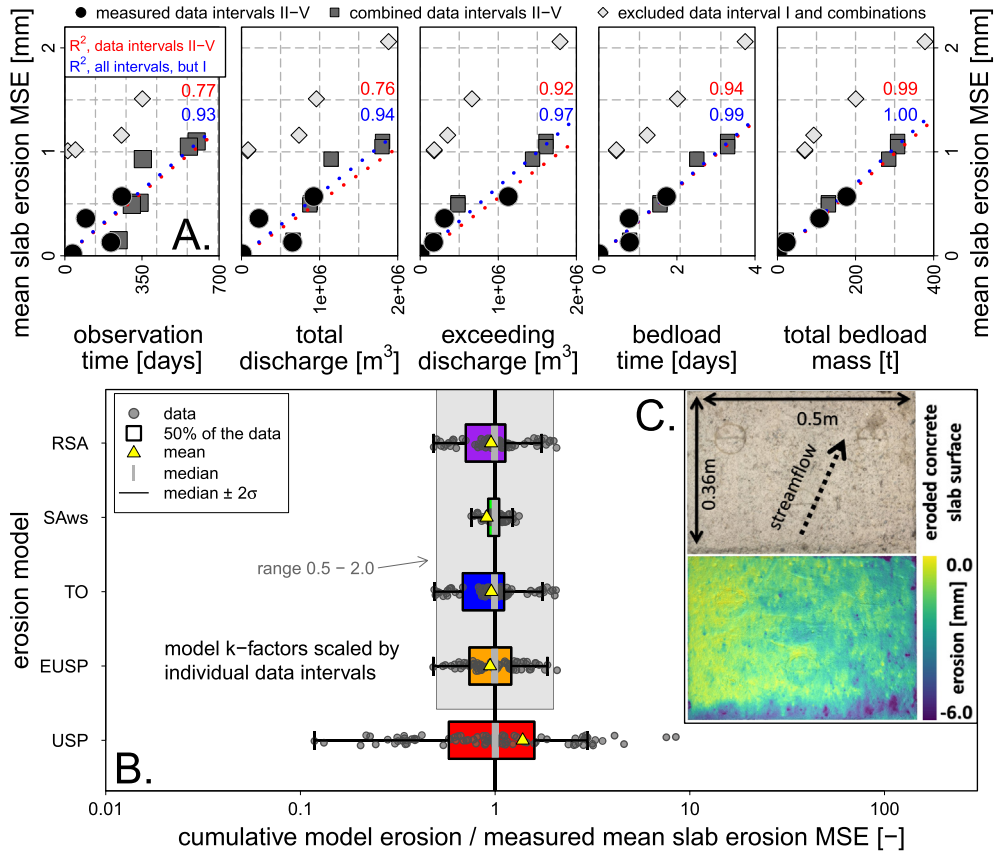

Figure 1. Month to annual time scale: (a) Erosion driver plausibility assessment, contrasting mean spatial slab erosion *MSE* with available parameters of the data intervals (Tables S1 and S2). Empirical linear regression's *R*-values are given as red numbers for the measured data intervals; for all of these and their combinations (except extended data interval I combinations), they are shown in blue. (b) Deviations of calibrated erosion model predictions relative to measured *MSE*. Each model's efficiency factor (*k*-factor) was first calibrated by one data interval and then erosion was predicted for all other data intervals, giving 90 predictions, respectively. Boxplot whiskers extend to 1.5 times the interquartile range from the box. (c) The inset shows a top view on the conrete slab after data interval V, indicating evolving surface morphology in the first and total spatial erosion measurements in the second panel.

3. Results

On the hour scale, the bedload-driven models (*TO*, *SAws*, and *RSA*) generally better matched the transient slab erosion pattern during the erosive events than the stream power-driven models (*USP* and *EUSP*; Figure S3). The former models did not reproduce individual erosion sensor steps, which are based on localized at-a-point bedload impacts, but followed the temporal erosion pattern during bedload transport peaks, in contrast to the smooth erosion predictions from integrating discharge-driven bed shear stress. Bedrock erodibility during data interval I was increased, which helped to resolve the erosion process in detail (Beer & Turowski, 2015). This, however, required exclusion of that initial period from further model assessment, because erodibility was not the same as in all other periods (Text S2).

At the month to annual scale (<1.5 years data), predictive quality for *MSE* increased in the sequence of general model driver data availability (time, discharge, bedload), at which the order of events seemed less important than their summed effect (Figure 1a). The worst empirical correlation (0.77) was found for observation time and the best for total bedload mass (0.99; red lines in Figure 1a for the combined data interval II–V). Including the combined data intervals improved and stabilized these correlations due to longer averaging times (blue lines Figure 1a). Consequently, models driven by bedload mass showed less than one order of magnitude deviation from *MSE* in modeling data interval erosion, with *SAws* performing best (Figure 1b). All but *USP* predicted zero erosion for data interval II lacking any bedload transport (Table S1).

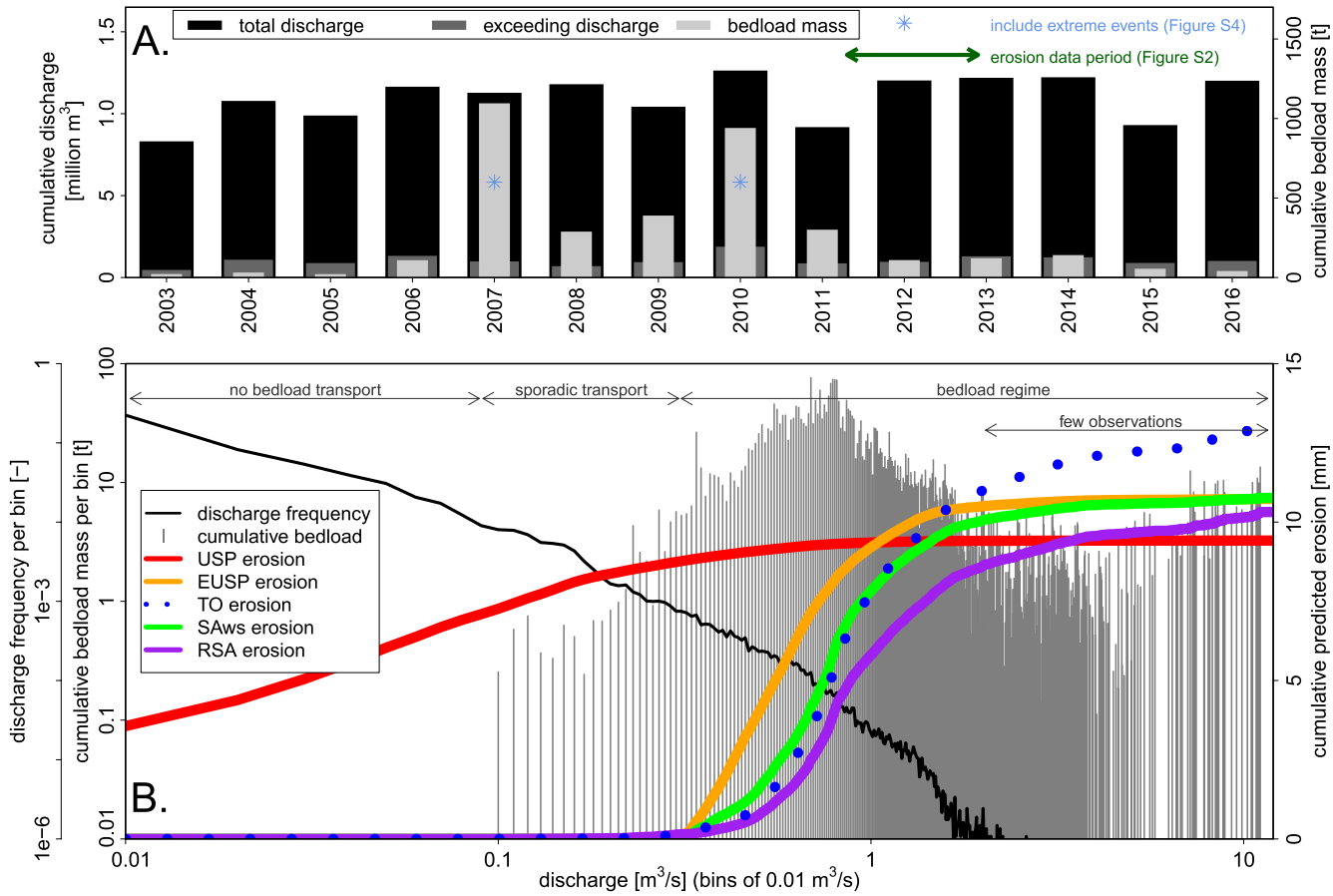

Figure 2. Decadal time scale: (a) annual sums of linked water discharge (exceeding discharge exceeds the bedload motion threshold) and bedload transport measurements taken in 1-min resolution, and (b) cumulative bedload mass and erosion predictions for 10*l* discharge bins of the data set in (a). The erosion models were scaled by their mean *k*-factors over the combined data interval II–V (Table 1). The dark green line in (a) constrains the period with additional slab erosion measurements (Figure S2A), and the light blue stars indicate the years containing the two exceptional flood events (Figure S4).

For the bedload-poor data interval III *USP* mispredicted by ± one order of magnitude, which diminished notably for *EUSP*.

Annual bedload mass transport at the Erlenbach is more variable than both the total and exceeding discharge (decadal scale; Figure 2a). Owing to long periods of low flow during the 14-year data set, 93% of *USP*-predicted erosion would have occurred for discharges below the onset of bedload motion (0.3 m^3/s, the onset of erosion predictions in all other models; Figure 2b). For the other models, more than 99% of the erosion occurred in less than 1% of time. Discharges exceeding the effective discharge (0.8 m^3/s) contribute less than 2.5% erosion for *USP*. For *EUSP* and *SAws*, 97.5% of erosion happened below discharges of 1- and 5-year recurrences, respectively (below 1.7 and 2.7 m^3/s). Over-decadal discharge recurrences both *TO* and *RSA* predictions rise constantly. Including bed cover (with a linear increase function for both *SAws* and *RSA* models) would dampen purely bedload-driven erosion (*TO*) by around 20% for 20-year discharges. Generally, both of these latter bedload-dependent models predict similar erosion rates as *EUSP*, exceed *USP* by over 10% and undershoot *TO* by 20%.

Extrapolating instantaneous erosivity to a centennial flood (corresponding to a peak discharge exceeding 16 m^3/s) resulted in up to four orders of magnitude difference in erosion rate predictions (exceeding 35 nm/min to 0.2 mm/min there; Figure 3a). The predicted peak instantaneous erosion rates for *SAws* and *RSA* happened at around 23 m^3/s(or a nearly 200-year flood) with 38% exposed bedrock, beyond which the other models predicted monotonously increasing erosion rates. Erosion damping by bed cover did not cause large deviations between bedload model predictions up to centennial floods, though transient full cover

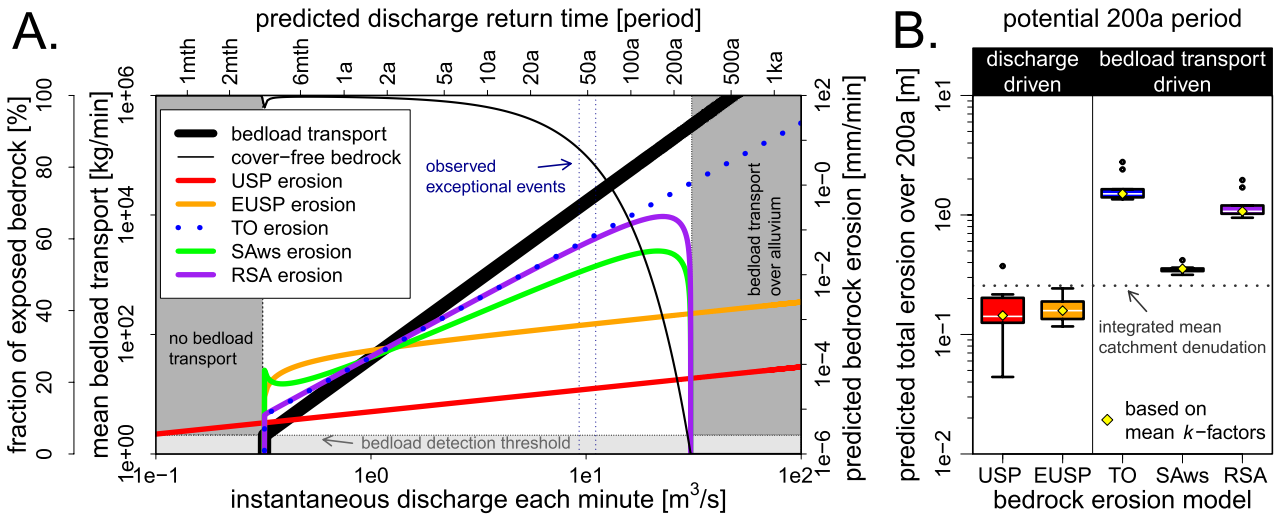

Figure 3. Centennial time scale: (a) Predicted erosion rates for instantaneous discharge and related mean bedload transport values. The discharge return times are based on an extrapolated gamma distribution of measured discharges over 32.5 years, and the mean bedload transport is based upon a regression on 16 years of bedload transport measurements. The erosion models were scaled by their mean *k*-factors over the combined data interval II–V (Table 1). The thin black line shows the predicted fraction of the bedrock streambed exposed to bedload. The dotted blue vertical lines indicate the largest measured discharges from the two exceptional events (Figure S4). (b) Total bedrock erosion predictions over 200 years of discharge and bedload transport, including a 200*a* flood event. Each erosion model was run with the 10*k*-factors possible from the month to annual time scale measurements; the yellow diamond represents the prediction using the mean *k*-factor (as used for panel a), respectively. Boxplot whiskers extend to 1.5 times the interquartile range from the box. The boxplots on the left side denote models driven by water discharge, and boxplots on the right side show models (additionally) driven by bedload transport. Mean catchment denudation prediction (gray dotted line) is from integrated mean sediment flux, as averaged over 25 years.

can already happen at low spatio-temporal scales, as was likely the case at the declining stages of both the observed exceptional events (Figure S4).

4. Discussion

For the sediment-starved conditions at the Erlenbach measuring site with usually negligible cover, bedrock erosion is linearly dependent on bedload mass at and exceeding the hour scale (Figure 1a). This confirms results from field and laboratory observations and from the abrasion process theory (Beer & Lamb, 2021; Beer & Turowski, 2015; Inoue et al., 2014; Jacobs & Hagmann, 2015; Johnson & Whipple, 2010; Mueller-Hagmann et al., 2020; Sklar & Dietrich, 2004), and it justifies extrapolating bedload-driven modeling beyond validation scales and cross-evaluation with pure discharge-driven erosion modeling. Generally uniform spatial slab erosion (Figure S2B) also verifies application of one-dimensional erosion models to predict spatial bed change (Mueller-Hagmann et al., 2020). Since information on bedload transport rates often is not available, bedload transport time as a general constraint on bedload flux provides an adequate substitute, at least for small events. It could be monitored, for example, by acoustic or seismic methods such as by a simple hydrophone (Barton et al., 2006; Geay et al., 2017). Restricting predictions to discharge exceeding the threshold of bedload transport resulted in a good predictive quality for *MSE*, since bedload flux generally scales with excess shear stress (or stream power), given sufficient available sediment (Phillips et al., 2018). Total discharge and observation time, though, had a lower goodness of fit ($R^2 < 0.8$) for the shorter single data intervals, but this diminished when accounting for the combined data intervals (blue correlations in Figure 1a).

Integrated at-a-point erosion from the discrete erosion sensor steps over time and varying forcing parameters generally agreed with mean spatial slab erosion. These measured steps hence reflect the transient spatial erosion of this patch (Figures S2B/C and S3). Thus, these local measurements (or likewise their predictions) seem representative of spatial surface change, given the homogeneous surface and bedload transport conditions. The increased slab erodibility during the first erosion event (an annual flood in data interval I) therefore allowed the erosion model exponent optimization analysis in a former study (Beer & Turowski, 2015). In the present study, the data interval I was excluded from the subsequent model performance assessment,

because there was a layer of highly erodible material on the slab's top due to concrete curing, which shifted all dependent *MSE* values (Figure 1a). The *USP* model both overpredicts non-erosive low discharges in between events (*USP*-jumps in between events, Figure S3) and underpredicts potentially highly erosive bedload transport rates during exceptional events (Figure S4). Thus, temporal scaling for the *USP* model is restricted, and its application range is determined by its calibration period. This deficit is reflected in its broadly deviating predictions when scaled by different parameter spaces (deviation of 1.5; Figure 1b). All other models revealed more reasonable prediction robustness over the annual scale (deviations of <= 0.5; i.e., kept the order of magnitude). So, their upscaling from the point to the patch scale (here the smooth and uniform slab surface; Figure 1c) and from the event to the year is feasible. Highest model robustness (deviation of 0.34) was obtained for *SAws*, followed by *EUSP*. The *RSA* and *TO* models slightly underpredicted measured erosion rates. This could be due to the influence of shear stress on bedload impacts, which they do not explicitly account for (Figure 1b; cf. Sklar & Dietrich, 2004).

Extrapolating model predictions beyond the erosion-measurement intervals revealed the critical role of non-linear increasing bedload transport with discharge in setting decadal erosion (Figure 2b). Given that bedrock erosion is driven by bedload impacts (Figure 1a), the stream-power models did not prove suitable for temporal upscaling. The *USP* model largely mispredicted at low clear-water discharges. Though *EUSP* performed better than *USP* at lower discharges, it does not capture the expected erosivity of large sediment-laden discharges exceeding bi-annual recurrence (Figure 3a). As a result, cumulative erosion predictions for the two exceptional events in 2007 and 2010 reached millimeters for the bedload-driven models, exceeding *USP* and *EUSP* predictions by two to three orders of magnitude and accounting for up to 12% of the total predicted erosion over the decade (Figure S4, Table S3). Both of these exceptional events showed similar cumulative discharge, resulting in equal *USP* and *EUSP* predictions. However, the first event transported twice as much bedload as the second, leading to double predicted erosion rates by the *TO* model, whereas *SAws* even predicted slightly smaller rates (Table S3). This highlights the relevance of bedload mechanistic modeling including bed cover, specifically during large events. For sediment-starved conditions as on the erosion slab, in exposed bedrock channels or on waterfall brinks, bedrock topography is strongly shaped—if not determined—by large erosive floods (e.g., Baker & Kale, 1998). This holds true even though mean erosion rates peak for bi-annual floods, which is similar to concepts advanced for alluvial rivers (Wolman & Miller, 1960). With abundant sediment supply, the streambed is cover-protected during high floods (Hartshorn et al., 2002), but the exposed bedrock erodes sufficiently fast to adjust the channel shape to hydraulic conditions (Anton et al., 2015; Lai et al., 2011; Larsen & Lamb, 2016; Phillips & Jerolmack, 2016). The *RSA* model captures both tools and cover effects here and is easier to apply than *SAws*, since it is independent of the onset of bedload motion.

The *k*-factor values for the annual scale (Table 1) are similar to literature values (Barnhart et al., 2020; Duval et al., 2004; Sklar & Dietrich, 2006; Snyder et al., 2000; Stock & Montgomery, 1999). Regarding the Erlenbach catchment, the concrete slab's tensile strength likely exceeded that of the local Flysch bedrock, that is, underestimating its erodibility. Further, we assumed a representative mean grain diameter of 0.02 m for the modeling, neglecting non-linear erosion rate scaling with increasing grain size (Beer & Lamb, 2021; Turowski et al., 2015), which would increase the bedload's erosivity for large discharges. In contrast, the slab is positioned in a steep, smooth, and exposed (i.e., cover-free) section not representative for the average river bed (Beer et al., 2015), which diminishes the actual erosivity of the flow. Still, taking the *TO* model as a simplification for *SAws*, the Erlenbach would need 280 t (106 m^3) of bedload to erode 1 mm of the slab, and by a mean annual bedload transport of 230 t, the slab would erode by 0.8 mm per year. This falls in the order of world's fast incising rivers (Koppes & Montgomery, 2009). Remarkably, the linear erosion-scaling with bedload implies the same instantaneous erosion rate for a centennial discharge (Figure 3a).

Point-calibrated bedload-models are a powerful tool to assess potential erosion rates for cover-free conditions over a range of temporal scales (Egholm et al., 2013; Snyder et al., 2003). Moreover, given a certain river incision rate and assuming a general lack of bed cover and a stable riverbed geometry, the required bedload transport mass could to first order be back-calculated from bulk erosion measurements, which allows the reconstruction of the catchment's history. Assuming a steady streambed configuration at the Erlenbach site, one meter of incision would require ~1200 ordinary years, or a 200*a* discharge lasting 24 h for the *TO* model (600 h for *SAws*). When integrating instantaneous erosion rates for minute-by-minute discharges up

to return times of a 200a event using the empirical relations (Figures S5 and 3a), the bedload-driven models predicted one order of magnitude higher erosion in comparison to the pure discharge-driven models, irrespective of their original scaling period (i.e., with a low prediction spread). Additional suspended load erosion may even increase these rates (Lamb et al., 2008). The *USP* and *EUSP* bi-centennial predictions did barely exceed the integrated mean catchment denudation rate (~0.13m, measured from the sediment flux over 1983–2008, neglecting centennial events; cf. Turowski et al., 2009; Figure 3b; this measure can be expected to be lower than the bedrock channel incision rate [Beer et al., 2017]). Explicitly accounting for bedload transport thus is critical in determining landscape evolution rates and topography. Generally, the actual spatial bedrock erosion pattern is controlled by the pattern of sediment availability that determines the interplay of the tools and cover effects (Figure S4), controls its temporal evolution (Anton et al., 2015; Beer et al., 2016, 2017; Lague, 2010; Turowski, 2018), and sets the frequency of large grain's erosive impacts on bare bedrock (Turowski et al., 2015). For sediment-starved conditions as on site, assuming stable channel beds as in bedrock sections, abrasion rates may thus be predictable using just the sediment's impact energy (Beer & Lamb, 2021), while plucking likely depends on shear stress (Lamb et al., 2015; Whipple et al., 2000).

5. Conclusions

Spatio-temporal upscaling of bedrock erosion models calibrated with local, short-term erosion measurements is reasonable for sediment-starved conditions lacking bedrock cover as at the Erlenbach observatory site, at waterfall brinks or in channels with exposed bedrock beds. The water discharge-driven unit stream power model including a threshold (*EUSP*) robustly predicts streamflow erosivity within its on-site calibration range, from minutes to years and at the patch scale, but not beyond. Due to the linear relation of bedload transport and erosion rate (tools effect), and the nonlinearity of discharge and bedload transport, large flood events can dominate the long-term bedrock incision and the evolution of the entire channel. Such events could cause orders of magnitude higher erosion rates than typical annual floods, as long as the bedrock bed remains exposed. Upscaling bedload tool- and cover-dependent predictions (*SAws* or *RSA* model) is appropriate to assess river erosivity exceeding centennial scales (Turowski, 2021). In addition, these models can be inverted to estimate long-term bedload supply from measured incision rates. Empirical stream power model calibrations strongly depend on their calibration period, implying that they cannot be applied across different time scales to simulate landscape evolution in mountain regions.

Data Availability Statement

The interval data sets of linked discharge, bedload transport, and bedrock erosion are made available via the following data repository: https://www.envidat.ch/dataset/linked-discharge-bedload-transport-and-bedrock-erosion-data-set. The longer-term data sets of bedload transport are accessible via https://www.envidat.ch/dataset/sediment-transport-observations-in-swiss-mountain-streams, and the long-term discharge data of the Erlenbach can be reached via https://www.envidat.ch/dataset/longterm-hydrological-observatory-alptal-central-switzerland.

Acknowledgments
The authors are grateful to Bruno Fritschi who designed, built, and maintained the facilities at the Erlenbach creek over decades and thank Dirk Rieke-Zapp, Lorenzo Campana, and Erich Müller for their invaluable support with spatial surveying, and James Kirchner and Ron Nativ for stimulating discussions and reviews of earlier manuscript versions. The authors very much appreciate the careful examination and assistance of Joel Scheingross and an anonymous reviewer that helped improve the paper. The Institute of Geological Science, University of Bern is acknowledged for lending their ALPA camera, and GOM International AG for providing their GOM ATOS III scanner. Concrete tensile strength was measured at ETH Zuerich. This study was supported by the SNF grant 200021_132163/1 to ARB, the University of Tuebingen, and GFZ Potsdam. Open access funding provided by ETH-Bereich Forschungsanstalten.

References

Anton, L., Mather, A. M., Stokes, M., Munoz-Martin, A., & De Vicente, G. (2015). Exceptional river gorge formation from unexceptional floods. *Nature Communications*, *6*, 7963–7963. https://doi.org/10.1038/ncomms8963

Auel, C., Albayrak, I., Sumi, T., & Boes, R. M. (2017). Sediment transport in high-speed flows over a fixed bed: 2. Particle impacts and abrasion prediction. *Earth Surface Processes and Landforms*, *42*, 1384–1396. https://doi.org/10.1002/esp.4132

Baker, V. R., & Kale, V. S. (1998). The role of extreme floods in shaping bedrock channels. In K. J. Tinkler, & E. E. Wohl (Eds.), *Rivers over rock: Fluvial processes in bedrock channels* (Vol. 107, pp. 30–60). American Geophysical Union. https://doi.org/10.1029/gm107p0153

Barnhart, K. R., Tucker, G. E., Doty, S., Shabe, C. M., Glade, R. C., Rossi, M. W., & Hill, M. C. (2020). Inverting topography for landscape evolution model process representation: 3. Determining parameter ranges for select mature geomorphic transport laws and connecting changes in fluvial erodibility to changes in climate. *Journal of Geophysical Research: Earth Surface*, *125*, e2019JF005287. https://doi.org/10.1029/2019JF005287

Barton, J. S., Slingerland, R. L., Pittman, S., & Gabrielson, T. B. (2006). *Passive acoustic monitoring of coarse bedload transport on the Trinity River* (pp. 627–634). Paper presented at Eighth Federal Interagency Sedimentation Conference, Advisory Committee on Water Information.

Beer, A. R., Kirchner, J. W., & Turowski, J. M. (2016). Graffiti for science—Erosion painting reveals spatially variable erosivity of sediment-laden flows. *Earth Surface Dynamics*, *4*, 885–894. https://doi.org/10.5194/esurf-4-885-2016

Beer, A. R., & Lamb, M. P. (2021). Abrasion regimes in fluvial bedrock incision. *Geology*, *49*(6), 682–686. https://doi.org/10.1130/G48466.1

Beer, A. R., & Turowski, J. M. (2015). Bedload transport controls bedrock erosion under sediment-starved conditions. *Earth Surface Dynamics*, *3*, 291–309. https://doi.org/10.5194/esurf-3-291-2015
Beer, A. R., Turowski, J. M., Fritschi, B., & Rieke-Zapp, D. (2015). Field instrumentation for high-resolution parallel monitoring of bedrock erosion and bedload transport. *Earth Surface Processes and Landforms*, *40*, 530–541. https://doi.org/10.1002/esp.3652
Beer, A. R., Turowski, J. M., & Kirchner, J. W. (2017). Spatial patterns of erosion in a bedrock gorge. *Journal of Geophysical Research: Earth Surface*, *122*, 191–214. https://doi.org/10.1002/2016JF003850
Chatanantavet, P., & Parker, G. (2009). Physically-based modeling of bedrock incision by abrasion, plucking, and macroabrasion. *Journal of Geophysical Research*, *114*, F04018. https://doi.org/10.1029/2008JF001044
Cook, K. L., Turowski, J. M., & Hovius, N. (2013). A demonstration of the importance of bedload transport for fluvial bedrock erosion and knickpoint propagation. *Earth Surface Processes and Landforms*, *38*(7), 683–695. https://doi.org/10.1002/esp.3313
Deal, E., Favre, A.-C., & Braun, J. (2017). Rainfall variability in the Himalayan orogen and its relevance to erosion processes. *Water Resources Research*, *53*, 4004–4021. https://doi.org/10.1002/2016WR020030\enleadertwodots
Duval, A., Kirby, E., & Burbank, D. (2004). Tectonic and lithologic controls on bedrock channel profiles and processes in coastal California. *Journal of Geophysical Research*, *109*, F03001. https://doi.org/10.1029/2003JF000086
Egholm, D. L., Knudsen, M. F., & Sandiford, M. (2013). Lifespan of mountain ranges scaled by feedbacks between landsliding and erosion by rivers. *Nature*, *498*, 475–478. https://doi.org/10.1038/nature12218
Gasparini, N. M., Whipple, X. X., & Bras, R. L. (2007). Predictions of steady state and transient landscape morphology using sediment-flux-dependent river incision models. *Journal of Geophysical Research*, *112*, F03S09. https://doi.org/10.1029/2006JF000567
Geay, T., Belleudy, P., Gervaise, C., habersack, H., Aigner, J., Kresiler, A., et al. (2017). Passive acoustic monitoring of bed load discharge in a large gravel bed river. *Journal of Geophysical Research: Earth Surface*, *122*, 528–545. https://doi.org/10.1002/2016JF004112
Hancock, G. S., Anderson, R. S., & Whipple, K. X. (1998). Beyod power: Bedrock river incision process and form. In K. J. Tinkler, & E. E. Wohl (Eds.), *Rivers over rock: Fluvial processes in bedrock channels* (Vol. 107, pp. 35–60). American Geophysical Union. https://doi.org/10.1029/gm107p0035
Hartshorn, K., Hovius, N., Dade, W. B., & Slingerland, R. L. (2002). Climate-driven bedrock incision in an active mountain belt. *Science*, *297*(5589), 2036–2038. https://doi.org/10.1126/science.1075078
Howard, A. D. (1994). Detachment-limited model of drainage basin evolution. *Water Resources Research*, *30*, 2261–2285. https://doi.org/10.1029/94WR00757
Howard, A. D., & Kerby, G. (1983). Channel changes in badlands. *Geological Society of America Bulletin*, *94*(6), 739–752. https://doi.org/10.1130/0016-7606(1983)94<739:CCIB>2.0.CO;2
Inoue, T., Izumi, N., Shimizu, Y., & Parker, G. (2014). Interaction among alluvial cover, bed roughness, and incision rate in purely bedrock and alluvial-bedrock channel. *Journal of Geophysical Research: Earth Surface*, *119*, 2123–2146. https://doi.org/10.1002/2014JF003133
Jacobs, F., & Hagmann, M. (2015). Sediment bypass tunnel Runcahez: Invert abrasion 1995-2014 (Technical report). *Proceedings of First International Workshop on Sediment Bypass Tunnels, VAW-Mitteilungen 232, Laboratory of Hydraulics, Hydrology and Glaciology (VAW)*, ETH Zurich.
Johnson, J. P., & Whipple, K. X. (2010). Evaluating the controls of shear stress, sediment supply, alluvial cover, and channel morphology on experimental bedrock incision rate. *Journal of Geophysical Research*, *115*, F02018. https://doi.org/10.1029/2009JF001335
Kirchner, J. W., Finkel, R. C., Riebe, C. S., Granger, D. E., Clayton, J. L., King, J. G., & Megahan, W. F. (2001). Mountain erosion over 10 yr, 10 k.y., and 10 m.y. time scales. *Geology*, *29*, 591–594. https://doi.org/10.1130/0091-7613(2001)029<0591:MEOYKY>2.0.CO;2
Koppes, M. N., & Montgomery, D. R. (2009). The relative efficacy of fluvial and glacial erosion over modern to orogenic timescales. *Nature Geoscience*, *2*, 644–647. https://doi.org/10.1038/NGEO616
Lague, D. (2010). Reduction of long-term bedrock incision efficiency by short-term alluvial cover intermittency. *Journal of Geophysical Research*, *115*, F02011. https://doi.org/10.1029/2008JF001210
Lague, D., Grave, A., & Davy, P. (2003). Laboratory experiments simulating the geomorphic response to tectonic uplift. *Journal of Geophysical Research*, *108*(B1). https://doi.org/10.1029/2002JB001785
Lai, Y. G., Greimann, B. P., & Wu, K. (2011). Soft bedrock erosion modeling with a two-dimensional depth-averaged model. *Journal of Hydraulic Engineering*, *137*(8), 804–814. https://doi.org/10.1061/(ASCE)HY.1943-7900.0000363
Lamb, M. P., Dietrich, W. E., & Skar, L. S. (2008). A model for fluvial bedrock incision by impacting suspended and bed load sediment. *Journal of Geophysical Research*, *113*, F03025. https://doi.org/10.1029/2007jf000915
Lamb, M. P., Finnegan, N. J., Scheingross, J., & Sklar, L. S. (2015). New insights into themechanics of fluvial bedrock erosion through flume experiments and theory. *Geomorphology*, *244*, 33–55. https://doi.org/10.1016/j.geomorph.2015.03.003
Larsen, I., & Lamb, M. P. (2016). Progressive incision of the Channeled Scablands by outburst floods. *Nature*, *538*, 694–697. https://doi.org/10.1038/nature19817
Mueller-Hagmann, M., Albayrak, I., Auel, C., & Boess, R. M. (2020). Field investigation on hydroabrasion in high-speed sediment-laden flows at sediment bypass tunnels. *Water*, *12*, 469. https://doi.org/10.3390/w12020469
Phillips, C. B., Hill, K. M., Paola, C., Singer, M. B., & Jerolmack, D. J. (2018). Effect of flood hydrograph duration, magnitude, and shape on bed load transport dynamics. *Geophysical Research Letters*, *45*, 8264–8271. https://doi.org/10.1029/2018GL078976
Phillips, C. B., & Jerolmack, D. J. (2016). Self-organization of river channels as a critical filter on climate signals. *Science*, *352*(6286), 694–697. https://doi.org/10.1126/science.aad3348
Rickenmann, D., Turowski, J. M., Fritschi, B., Klaiber, A., & Ludwig, A. (2012). Bedload transport measurements at the Erlenbach stream with geophones and automated basket samplers. *Earth Surface Processes and Landforms*, *37*, 1000–1011. https://doi.org/10.1002/esp.3225
Seidl, M. A., & Dietrich, W. E. (1992). The problem of channel erosion into bedrock. *Catena Supplement*, *23*, 11–124.
Sklar, L. S., & Dietrich, W. E. (2004). A mechanistic model for river incision into bedrock by saltating bed load. *Water Resources Research*, *40*, W06301. https://doi.org/10.1029/2003WR002496
Sklar, L. S., & Dietrich, W. E. (2006). The role of sediment in controlling steady-state bedrock channel slope: Implications of the saltation-abrasion incision model. *Geomorphology*, *82*, 58–83. https://doi.org/10.1016/j.geomorph.2005.08.019
Snyder, N. P., Whipple, K. X., Tucker, G. E., & Merritts, D. J. (2000). Landscape response to tectonic forcing: Digital elevation model analysis of stream proles in the Mendocino triple junction region, northern California. *Geological Society of America Bulletin*, *112*, 1250–1263. https://doi.org/10.1130/0016-7606(2000)112<1250:lrttfd>2.0.co;2
Snyder, N. P., Whipple, K. X., Tucker, G. E., & Merritts, D. J. (2003). Importance of a stochastic distribution of floods and erosion thresholds in the bedrock river incision problem. *Journal of Geophysical Research*, *108*(B2). https://doi.org/10.1029/2001JB001655

Stock, J. D., & Montgomery, D. R. (1999). Geologic constraints on bedrock river incision using the stream power law. *Journal of Geophysical Research*, *104*(B3), 4983–4993. https://doi.org/10.1029/98JB02139

Sunamura, T. (2018). A fundamental equation for describing the rate of bedrock erosion by sediment-laden fluid flows in fluvial, coastal, and aeolian environments. *Earth Surface Processes and Landforms*, *43*(15), 3022–3041. https://doi.org/10.1002/esp.4467

Tomkin, J. H., Brandon, M. T., Pazzaglia, F. J., Barbour, J. R., & Willett, S. D. (2003). Quantitative testing of bedrock incision models for the clearwater river, NW, Washington State. *Journal of Geophysical Research*, *108*(B6). https://doi.org/10.1029/2001JB000862

Turowski, J. M. (2012). Semi-alluvial channels. In M. Church, A. G. Roy, & P. M. Biron (Eds.), *Gravel-bed rivers: Processes, tools environments* (pp. 401–418). Whiley-Blackwell.

Turowski, J. M. (2018). Alluvial cover controlling the width, slope and sinuosity of bedrock channels. *Earth Surface Dynamics*, *6*, 29–48. https://doi.org/10.5194/esurf-6-29-2018

Turowski, J. M. (2021). Upscaling sediment-flux-dependent fluvial bedrock incision to long timescales. *Journal of Geophysical Research: Earth Surface*, *126*, e2020JF005880. https://doi.org/10.1029/2020JF005880

Turowski, J. M., Badoux, A., Leuzinger, J., & Hegglin, R. (2013). Large floods, alluvial overprint, and bedrock erosion. *Earth Surface Processes and Landforms*, *38*, 947–958. https://doi.org/10.1002/esp.3341

Turowski, J. M., Wyss, C. R., & Beer, A. R. (2015). Grain size effects on energy delivery to the stream bed and links to bedrock erosion. *Geophysical Research Letters*, *42*, 1775–1780. https://doi.org/10.1002/2015GL063159

Turowski, J. M., Yager, E. M., Badoux, A., Rickenmann, D., & Molnar, P. (2009). The impact of exceptional events on erosion, bedload transport and channel stability in a step-pool channel. *Earth Surface Processes and Landforms*, *34*, 1661–1673. https://doi.org/10.1002/esp.1855

van der Beek, P., & Bishop, P. (2003). Cenozoic river profile development in the upper Lachlan catchment (SE Australia) as a test of quantitative fluvial incision models. *Journal of Geophysical Research*, *108*(B6), 2309. https://doi.org/10.1029/2002JB002125

Whipple, K. X., DiBiase, V., & Crosby, B. T. (2013). Bedrock rivers. In A. Switzer, & D. M. Kennedy (Eds.), *Treatise in geomorphology: Methods in geomorphology* (Vol. 9.28, pp. 550–573). Elsevier. https://doi.org/10.1016/b978-0-12-374739-6.00254-2

Whipple, K. X., Hancock, G. S., & Anderson, R. S. (2000). River incision into bedrock: Mechanics and relative efficacy of plucking, abrasion, and cavitation. *Geological Society of America Bulletin*, *112*(3), 490–503. https://doi.org/10.1130/0016-7606(2000)112<490:RIIBMA>2.0.CO;2

Whipple, K. X., & Tucker, G. E. (1999). Dynamics of the stream-power river incision model: Implications for height limits of mountain ranges, landscape response timescales, and research needs. *Journal of Geophysical Research*, *104*(B8), 17661–17674. https://doi.org/10.1029/1999JB900120

Wolman, M. G., & Miller, J. P. (1960). Magnitude and frequency of forces in geomorphic processes. *The Journal of Geology*, *68*(1), 54–74. https://doi.org/10.1086/626637

References From the Supporting Information

Barry, J. J., Buffington, J. M., & King, J. D. (2004). A general power equation for predicting bed load transport rates in gravel bed rivers. *Water Resources Research*, *40*, W10401. https://doi.org/10.1029/2004WR003190

Crave, A., & Davy, P. (2001). A stochastic "precipiton" model for simulating erosion/sedimentation dynamics. *Computers & Geosciences*, *27*, 815–827. https://doi.org/10.1016/S0098-3004(00)00167-9

Lague, D., Brodu, N., & Leroux, J. (2013). Accurate 3d comparison of complex topography with terrestrial laser scanner: Application to the Rangitikei canyon (N-Z). *ISPRS Journal of Photogrammetry and Remote Sensing*, *82*, 10–26. https://doi.org/10.1016/j.isprsjprs.2013.04.009

Lague, D., Hovius, N., & Davy, P. (2005). Discharge, discharge variability, and the bedrock channel profile. *Journal of Geophysical Research*, *110*, F04006. https://doi.org/10.1029/2004JF000259

Rickenmann, D. (2020). Effect of sediment supply on cyclic fluctuations of the disequilibrium ratio and threshold transport discharge, inferred from bedload transport measurements over 27 years at the Swiss Erlenbach stream. *Water Resources Research*, *56*, e2020WR027741. https://doi.org/10.1029/2020WR027741

Rieke-Zapp, D. H., Beer, A. R., Turowski, J. M., & Campana, L. (2012). *In situ measurement of bedrock erosion* (Vol. XXXIX-B5, pp. 429–433). ISPRS – International Archives of the Photogrammetry, Remote Sensing and Spatial Information Sciences. https://doi.org/10.5194/isprsarchives-XXXIX-B5-429-2012